

Enzymatic Modification of a Model Homogalacturonan with the Thermally Tolerant Pectin Methyltransferase from *Citrus*: 1. Nanostructural Characterization, Enzyme Mode of Action, and Effect of pH

Randall G. Cameron,^{*,†} Gary A. Luzio,[†] Prasanna Vasu,[‡] Brett J. Savary,^{‡,§} and Martin A. K. Williams^{||,⊥,¶}

[†]Citrus and Subtropical Products Laboratory, Agricultural Research Service, United States Department of Agriculture, 600 Avenue S., Northwest, Winter Haven, Florida 33881, United States

[‡]Arkansas Biosciences Institute, Arkansas State University, Post Office Box 639, State University, Arkansas 72467, United States

[§]College of Agriculture and Technology, Arkansas State University, Jonesboro, Arkansas 72467, United States

^{||}Institute of Fundamental Sciences, Massey University, Science Tower C4.09, Turitea Site, Palmerston North Campus, Private Bag 11222, Palmerston North 4442, New Zealand

[⊥]MacDiarmid Institute for Advanced Materials and Nanotechnology, Victoria University of Wellington, Post Office Box 600, Wellington 6140, New Zealand

[¶]Riddett Institute, Massey University, Private Bag 11222, Palmerston North 4442, New Zealand

ABSTRACT: Methyl ester distribution in pectin homogalacturonan has a major influence on functionality. Enzymatic engineering of the pectin nanostructure for tailoring functionality can expand the role of pectin as a food-formulating agent and the use of *in situ* modification in prepared foods. We report on the mode of action of a unique citrus thermally tolerant pectin methyltransferase (TT-PME) and the nanostructural modifications that it produces. The enzyme was used to produce a controlled demethylesterification series from a model homogalacturonan. Oligogalacturonides released from the resulting demethylesterified blocks introduced by TT-PME using a limited endopolygalacturonase digestion were separated and quantified by high-pressure anion-exchange chromatography (HPAEC) coupled to an evaporative light-scattering detector (ELSD). The results were consistent with the predictions of a numerical simulation, which assumed a multiple-attack mechanism and a degree of processivity ~ 10 , at both pH 4.5 and 7.5. The average demethylesterified block size (0.6–2.8 nm) and number of average-sized blocks per molecule (0.8–1.9) differed, depending upon pH of the enzyme treatment. The mode of action of this enzyme and consequent nanostructural modifications of pectin differ from a previously characterized citrus salt-independent pectin methyltransferase (SI-PME).

KEYWORDS: Pectin, nanostructure, pectin methyltransferase, thermally tolerant pectin methyltransferase, degree of processivity, mode of action, endopolygalacturonase, EPG, polysaccharide, homogalacturonan

INTRODUCTION

Organoleptic qualities of processed and formulated foods are primary determinants of consumer acceptability. Examples of product quality mediated by the pectin molecule nanostructure are stabilization of milk proteins in acid dairy drinks, generation of texture in jams and jellies, control of cloud loss in cloudy fruit juices, and use of ionic interactions to produce a firmer texture in fruits and vegetables. Texture is a major determinant for consumer acceptance of processed fruits and vegetables.^{1–3} A key contributing component to texture in these processed and formulated foods is pectin, which is a structural polysaccharide found in both plant primary cell walls and middle lamella.^{5–8} The major structural domain in pectin is homogalacturonan (HG), a linear polymer of galacturonic acid (GalA), estimated to range from 75 to 250 residues in length,⁹ equivalent to approximately 30–120 nm in length,^{10,11} which is variably methylated at the C6-carboxyl functional group.¹² Reduction in the degree of methylation (DM) of pectin following chemical or enzymatic treatment can influence firmness via calcium–pectin interactions.¹ Fraeye et al.⁴ discussed the importance of the

demethylesterification pattern as well as the total extent of demethylesterification (i.e., DM) and concluded that both can have a large effect on the texture of processed foods. Blockwise demethylesterification observed with plant pectin methyltransferases (pPMEs), which have alkaline pH optima, is more likely to contribute to calcium cross-linking than random demethylesterification associated with fungal pectin methyltransferases (PMEs) that usually have an acidic pH optima. A second major role for modified pectin is the stabilization of acidic dairy drinks, where the pectin forms a multi-layer coating around aggregates of casein micelles, preventing their sedimentation.¹³ Although pectin marketed for gelation is generally labeled as either high (>50% DM) or low (<50% DM) methoxyl pectin, Willats et al.¹⁴ also demonstrated that both the demethylesterification pattern and DM influence gel properties. Pectin also interacts with food

Received: December 16, 2010

Revised: February 1, 2011

Accepted: February 8, 2011

Published: March 02, 2011

matrix materials to affect aroma release and perception^{15,16} and has been under investigation as an encapsulant for colonic drug delivery¹⁷ and folic acid delivery.¹⁸

Because the functionality of pectin is dependent upon the amount and distribution of ion-binding groups in the HG region, the development of a technology to rationally engineer these structural attributes is desirable. Such a technology requires an ability to predictably introduce, characterize, and subsequently map the non-random, demethylesterified nanostructure, at the level of a single molecule and population of molecules. This would enable manipulation of the functionality of pectin and expand its use, both *in situ* and as a formulating agent that has optimum and predictable physical properties targeted to a particular application.

Recently, we have demonstrated the feasibility of enzymatically modifying pectin and characterizing the introduced nanostructure, correlating resulting functionality to the structure and modeling the enzyme mode of action under different reaction conditions.^{19,20} A model HG was demethylesterified with a salt-independent pectin methyltransferase (SI-PME) from *Citrus sinensis* fruit tissue²¹ to produce a demethylesterification series ranging from 90 to 50% DM. One set demethylesterified at pH 7.5, and another set demethylesterified at pH 4.5. These demethylated pectins underwent a limited digestion with a commercially available endopolygalacturonase (EPG) to release oligogalacturonides from the demethylesterified blocks (DMBs) introduced by the PME. A computer simulation of EPG digestion patterns^{19,22} was then used in conjunction with further mathematical modeling to probe the PME mode of action and degree of processivity (p), the number of contiguous GalA residues demethylated before the enzyme moves to a new catalytic site. In summary, these data suggested that average DMB length and number per molecule, as well as the final DM, could be manipulated by reaction conditions (pH). Additionally, pH also appeared to affect the PME mode of action, and on the basis of the data, we hypothesized that the PME used possessed a variable degree of processivity that increased as the DM decreased. These structurally well-characterized pectins were then evaluated by functional testing in terms of rheological properties and calcium sensitivity. It was concluded that, as hypothesized, the DMB size and number of DMBs per molecule, both of which could be manipulated, need to be considered to account for the manifested pectin functionality.²⁰

Here we report on the characterization of the nanostructural features introduced into a model HG during demethylesterification with the thermally tolerant pectin methyltransferase (TT-PME) present in citrus fruit tissue^{23–27} and the mode of action of the enzyme at pH 4.5 and 7.5. TT-PME is a structurally unique PME that has only been identified from tissues of *Citrus* spp. It has a much higher degree of thermal tolerance than reported for other PMEs and also retains activity at the pH of citrus juices (~3.7).^{24,26} TT-PME is observed as two glycoforms that migrate as 46 and 56 kDa peptides with denaturing electrophoresis (Savary et al., manuscript in preparation). We also compare the findings from the citrus TT-PME to those previously obtained with the thermally labile citrus SI-PME.¹⁹

MATERIALS AND METHODS

Chemicals. All chemicals were purchased from Sigma–Aldrich (St. Louis, MO), unless otherwise indicated. Endopolygalacturonase (EPG-M2) was purchased from Megazyme International Limited (Bray, Ireland; Lot 00801).

Enzyme Isolation. Monocomponent preparations of TT-PME were prepared with few modifications according to the procedure developed by Savary et al. (manuscript in preparation). Briefly, *Citrus sinensis* var. Valencia finisher pulp, obtained from a local citrus juice processor, was washed 2 times with a 3:1 ratio (w/v) of a 20 mM NaOAc and 50 mM NaCl solution, stirring at 4 °C for 60 min/wash. The pulp suspension was filtered through Miracloth (EMD Chemicals, Gibbstown, NJ) and then extracted with 3 volumes (w/v) of 20 mM NaOAc and 500 mM NaCl at pH 5.0. Lithium azide was added to 0.02% (w/v) as a preservative. The suspension was stirred overnight at 4 °C. Solids were removed by filtration over Miracloth, and the supernatant, containing PME activity, was first filtered through a 1.5 μ m glass microfiber filter and then an Acropak 500 Capsule (0.8/0.2 μ m; Pall Corporation, Ann Arbor, MI). The filtered extract was concentrated 10-fold with a Pall Centramate 10 kDa molecular-weight cut-off (MWCO) tangential flow filtration device. After concentration, the solution was diluted 2.5-fold with 20 mM sodium phosphate buffer at pH 7.0 to give a final NaCl concentration of 200 mM. Pectates were removed by batch adsorption to DEAE-Sepharose previously equilibrated with 200 mM NaCl in 20 mM sodium phosphate buffer at pH 7.0, stirred overnight at 4 °C, then filtered with 1.5 μ m glass microfiber filter to remove the DEAE resin. The filtrate was concentrated 10-fold with the Pall Centramate 10 kDa MWCO tangential flow filtration device and then heated at 70 °C in a water bath for 30 min to inactivate all but TT-PME. TT-PME activity present in the extract was determined as previously described.²⁴

Pectin Demethylation. Pectin [86% anhydrous galacturonic acid (AGA), 94% DM, containing minor amounts of galactose] was made to a final solution of 1% in 0.2 M LiCl at pH 4.5 or 7.5 (pH adjusted with LiOH). A total of 1 L of the pectin solution was added to a 5 L water-jacketed stirred bioreactor and equilibrated at 30 °C.¹⁹ A sufficient volume of enzyme was added to equal 175 units of PME activity (as measured at 30 °C), and the pH was maintained at either 4.5 or 7.5 with a radiometer PHM290 pH-stat controller (Radiometer Analytical, Villeurbanne Cedex, France) using 1 M LiOH as the titrant. When sufficient titrant was added to indicate that the desired DM had been reached, the reaction was quenched by rapidly (~5 s) draining the reactor contents into a vessel containing two volumes of acidified 95% ethanol (pH 3.8) at 37 °C, precipitating the pectin and inactivating the enzyme. The precipitated pectin was stored at 4 °C to facilitate further precipitation. The precipitated pectin was centrifuged (23400g for 30 min at 4 °C), and the supernatant was discarded. The pellet was placed in liquid nitrogen (forming small spheres), lyophilized, and then comminuted in a small kitchen-style mill. The comminuted pectin was frozen at –80 °C in a desiccated container.

EPG Digests. Demethylesterified pectins at 0.25% (w/v) in 50 mM lithium acetate (pH 5.5) and 0.02% lithium azide (w/v) were equilibrated at 30 °C in a benchtop incubator with stirring and digested with EPG-M2 (0.1 unit mL⁻¹) for 10 min. Preliminary results (data not shown) demonstrated that these conditions released unmethylated oligomers without significant hydrolysis of the released oligomer products. EPG activity was quenched by pipetting the solution into a beaker containing 160 μ L of concentrated HCl to lower the pH to ~2, then microwaving the sample for 10–12 s to boiling, and finally immersing the sample in a boiling water bath for 10 min.

Chromatography. Weight average (M_w) and number average (M_n) molecular weights for the parent pectin were determined by size-exclusion–multi-angle laser light scattering (SEC–MALLS; Wyatt Technologies, Santa Barbara, CA).¹⁹ Compositional analysis of the parent pectin was performed by hydrolysis with pectinases (P2611, Sigma-Aldrich), followed by quantitative analysis of sugars by anion-exchange chromatography using dilute sodium hydroxide and sodium acetate buffer systems coupled to a pulsed amperometric detector.²⁸

Oligomers released by the limited EPG digestion of demethylated pectins were separated and quantified by high-pressure anion-exchange

chromatography (HPAEC) coupled to an evaporative light-scattering detector (ELSD).^{19,29} For oligomers with a relatively low (<12) degree of polymerization (DP), 50 μL injections were made, while 250 μL injections were used for oligomers with a DP > 12. Three replicate injections were used for each estimate. Masses for each oligomer (GalA_n , where n is the number of demethylesterified GalA residues in the oligomer) were estimated using a pooled calibration curve constructed using GalA_6 and GalA_{13} . No significant differences between the slopes (F , 0.222 78; DFn , 1; DFd , 26; and p , 0.6409) and intercepts (F , 0.511 73; DFn , 1; DFd , 27; and p , 0.4805) for the individual calibration curves (each curve contained five concentration levels, and each level was replicated 3 times) were observed when tested using an ANCOVA test (performed using GraphPad Prism, version 4.03, for Windows, Graph-Pad Software, San Diego, CA, www.graphpad.com). Oligomer mass estimates were converted to molar concentration as previously described.¹⁹

Mass concentrations for each GalA_n were used to calculate GalA_n molar concentration per milliliter (C_n). The number average molecular weight obtained from SEC-MALLS was used to estimate the molar concentration of pectin per milliliter (C_p). Equation 1 was used to estimate the average number of DMBs released from a molecule of length n (\bar{B}_n) for each oligomer of GalA_n .

$$\bar{B}_n = \frac{C_n}{C_p} \quad (1)$$

The average number of blocks per molecule (\bar{B}) is the sum of the average number of DMBs of size n .

$$\bar{B} = \sum_{n=3}^z \bar{B}_n \quad (2)$$

The average DMB size (\bar{BS}) released was estimated according to eq 3.

$$\bar{BS} = \frac{\sum_{n=3}^z n\bar{B}_n}{\bar{B}} \quad (3)$$

The number of blocks of the average block size (\bar{BS}) per molecule (\bar{BN}) was estimated according to eq 4.

$$\bar{BN} = \frac{\bar{B}}{\bar{BS}} \quad (4)$$

Statistical analyses of the results were performed in Excel 2007 (Microsoft, Redmond, WA) and GraphPad Prism. The 70%, pH 4.5 pectin was lost; therefore, data for the 70% and pH 7.5 sample was excluded.

Mathematical Modeling. A set of one-dimensional arrays was used to model a population of polymer molecules. The lengths of the arrays were selected so that the population had a Gaussian distribution of DP with a defined width and mean value. The array elements represented the esterification state of each sugar ring and were assigned so that the population had a Gaussian distribution of the chain-averaged DM between chains with a defined width and mean value. A number average DM of 94 [full width at half height (fwhh) = 8] and DP of 140 (fwhh = 40) were used for all simulations described, chosen to approximate the experimentally measured distributions of the starting polymer employed in the experimental study. Subsequently, various de-esterification algorithms were applied to the starting substrate set until a specified end point was achieved, where the DM had been reduced to a value for which experimental data were available. When the degree of multiple attack was selected,^{14,30–34} both random and processive modes of action could be investigated.

After substrate modification, the new intramolecular distribution of methylesters (E) could be monitored *in silico*. While this distribution cannot be measured directly experimentally, it has been shown that the relative amount of oligogalacturonides of different DPs released in a

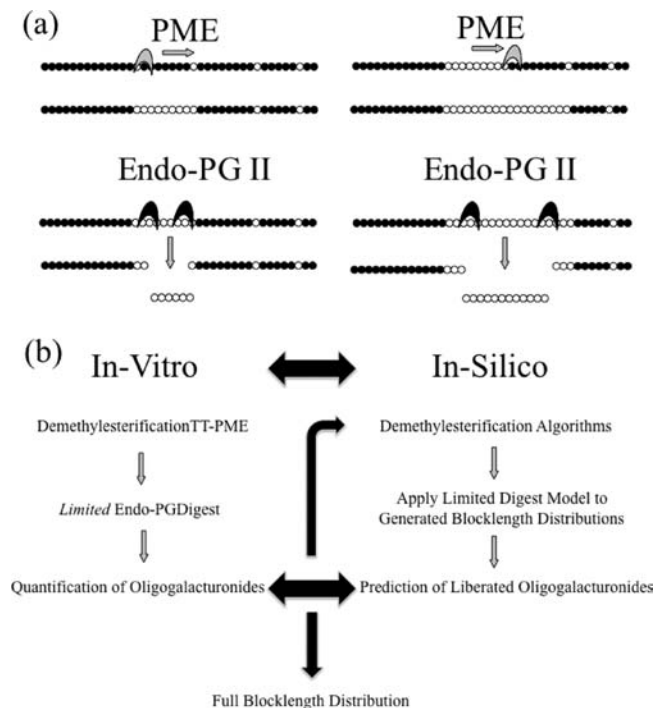


Figure 1. (a) Schematic of TT-PME and EPG processing of model HG substrates, showing the introduction of demethylesterified blocks by PME and the subsequent random release of oligogalacturonides of different length, whose concentrations are measured experimentally. (b) Schematic of the modeling procedure.

limited EPG digest is closely related to the unmethylesterified GalA (G) block lengths present in the original substrate.¹⁹ Hence, for the different models of PME enzyme action investigated, the question as to how the differences in the generated unmethylesterified GalA block lengths in the population would be mirrored in the distribution of DPs of oligogalacturonides released by a limited EPG digestion was addressed by calculation. Assuming that the EPG acts randomly within an unesterified block, the relative probability of removing a k -mer from a block n long is given by

$$\frac{(n-2) - k + 1}{((n-2)^2 + (n-2))/2} \quad (5)$$

The factor of $(n-2)$ arises from the assumption that the EPG active site requires two unmethylated residues, and whatever cuts are made, an unmethylesterified residue is always left on either side (i.e., from a block of eight unmethylated residues, an oligomer of six would be the largest extracted). The numerical simulations of the substrate after PME action give the relative numbers, N , of the different initial unmethylesterified GalA blocks of varied length, $\text{E}-(\text{G})_n-\text{E}$, in the polymer population, and eq 5 gives a way of estimating, for each of those, the relative amount of oligogalacturonides of different DPs liberated by a limited EPG digestion. Hence, the relative total number of unmethylesterified GalA k -mers released in such a digestion can be written as

$$\sum_{n=k+2}^{n=\text{chain length}} \frac{N(\text{E}-(\text{G})_n-\text{E})[(n-2) - k + 1]}{\{[(n-2)^2 + (n-2)]/2\}} \quad (6)$$

This allows for predictions to be made for each PME model that can be compared directly to experimental data. With such a simulation methodology in hand, then (i) different PME models can be assessed for their ability to describe the results of EPG-limited digest experiments of the

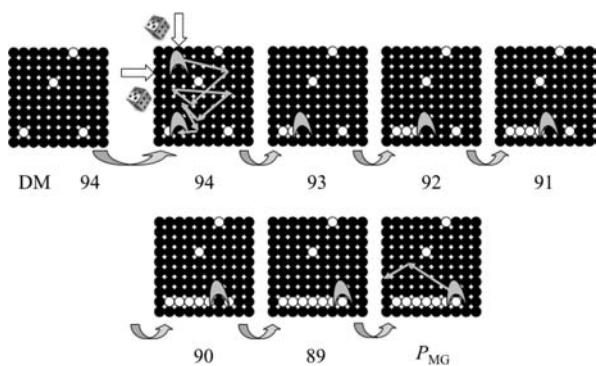


Figure 2. Schematic representation of the operation of the pPME model shown for a simplified case of 10 chains, each 10 residues in length. The “enzyme” can be seen diffusing around until finding a binding site, traveling along a number of methylesterified residues, demethylesterifying them, then detaching from the chain upon encountering an unmethylesterified residue, and finally continuing to walk around the two-dimensional (residue label \times chain label) array.

PME-engineered substrates and, (ii) for the model that best describes the experimental results, the full unmethylesterified GalA block length distribution of the predigested PME-generated polymers can be displayed. The strategy is summarized in panels a and b of Figure 1.

The algorithm used to model the PME mode of action is based on that recently used to model intermolecular DM distributions in HGs,³⁵ with a simple addition that a maximum processivity of the enzyme was also introduced. Slightly more elaborate enzyme models that incorporate information regarding how methylesterified residues might be incorporated more or less favorably into different enzyme subsites³⁵ can easily be constructed within the simulation framework and are the subject of current work. Such extensions are likely to be particularly useful in investigating cases in which pPME action is initiated on randomly demethylesterified starting substrates of lower DM, which will hence exhibit a larger variety of tetra- or pentameric sugar residue sequences within the binding cleft length. The substrates described here, however, being of very high initial DM, exhibit a limited number of possible residue patterns extending the length of the binding cleft and, thus, are largely insensitive to such further elaborations. As mentioned above, a further feature, maximum processivity, was also found to be useful to be introduced here, so that the processing nature of the enzyme could also be limited to a particular number of residues (p) if desired.

When a single enzyme–substrate interaction is over, then further searching of a two-dimensional (residue label \times chain label) array for binding sites continues in two possible modes: (i) simple random selection of another array element or (ii) a pseudo-diffusive process, in which the “enzyme” describes a random walk over other sites. In the simulations described herein, such a walk is implemented for 170 steps, before another “enzyme” (another randomly selected starting point) takes over, corresponding approximately to the experimental conditions of there being one enzyme for 170 polysaccharide chains. Figure 2 shows a schematic example of this model for a simplified case of 10 chains, each 10 residues in length. The “enzyme” can be visualized as finding a binding site, traveling along a number of methylesterified residues, demethylesterifying them as it goes, then detaching from the chain upon encountering an unmethylesterified residue, and finally continuing to walk around the two-dimensional (residue label \times chain label) array.

RESULTS AND DISCUSSION

As determined by SEC–MALLS, the M_w for the parent pectin (i.e., the model HG) was 53 060 and the number average molecular weight (M_n) was 27 613. GalA (93%) and galactose

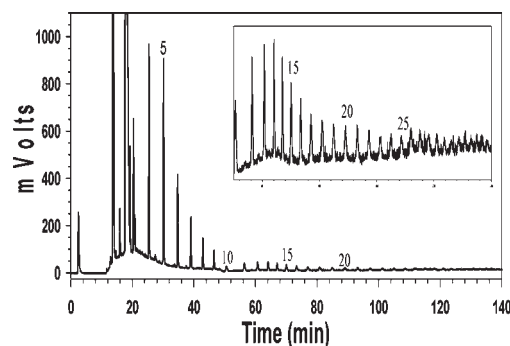


Figure 3. Representative HPAEC–ELSD chromatogram of oligogalacturonides released after a 10 min EPG digest of the pH 7.5 and 60% DM pectins. Numbers indicate oligomer DP of the corresponding peak. The inset is a zoom of the chromatogram for the indicated region.

(7%) were the only sugars detected; the lack of any rhamnose indicates the parent pectin is a HG. The relatively low value for M_n and the high reported DM value indicates that this pectin was likely produced by chemical methylation with an acidified methanol procedure, as detailed by Rosenbohm et al.,³⁶ which resulted in a loss of molecular weight. This treatment would also lead to cleavage of the HG from rhamnagalacturonan I, which would account for the lack of rhamnose in the parent pectin. Using the value for M_n and an average molecular weight of 189.34 (on the basis of a DM value of 94%) for AGA gives an average DP of 146 (\sim 65 nm) for this HG. This is larger than values of 71–92 reported by Ralet et al.¹⁰ or 72–100 by Thibault et al.⁹ Additionally, Ralet et al.¹⁰ reported that they restricted the elution volume range used for integration to the region of their calibration curve, which eliminated possible affects from aggregation and low light scattering. Therefore, the calibration curve used for the data presented here may have contained a broader molecular weight range that could account for the increase in observed M_n and resulting DP of the HG.

The probability of a pre-existing DMB being present in this parent pectin of the minimal block size needed for relatively rapid EPG cleavage^{37,38} was very low, only approximately 0.004 for a GalA₂, and this would, in any case, only fragment the HG and not release a GalA_n oligomer. Indeed, no oligomers were released from the parent 94% DM pectin following the 10 min EPG digest, and consequently, oligomers released from the demethylated pectins were considered to be a result of the demethylation with TT-PME. Oligogalacturonides were released from all of the demethylesterified pectins (Figures 3 and 4 and Table 1) by a limited digestion with EPG. Partially methylated fragments eluted between 10 and 25 min as a broad hump (Figure 3). The unmethylesterified GalAs in these oligomers were either randomly distributed, uncleaved terminal GalAs or likely in contiguous blocks too small for cleavage by the EPG ($<$ GalA₄).³⁸ Retention time of GalA reference oligomers was made with purchased standards and individual purified oligomers subsequently identified by high-performance liquid chromatography–mass spectrometry (HPLC–MS) and SEC–MALLS.¹⁹ The observed distribution of released unmethylated blocks can be related to the actual block sizes present in the undigested molecules through extensive mathematical modeling presented here. Small oligomers are the numerically most abundant oligomers released from the demethylated pectin by EPG (Figure 4). Although the possibility of releasing oligomers by secondary digestion cannot be discounted, the frequency of small oligomers

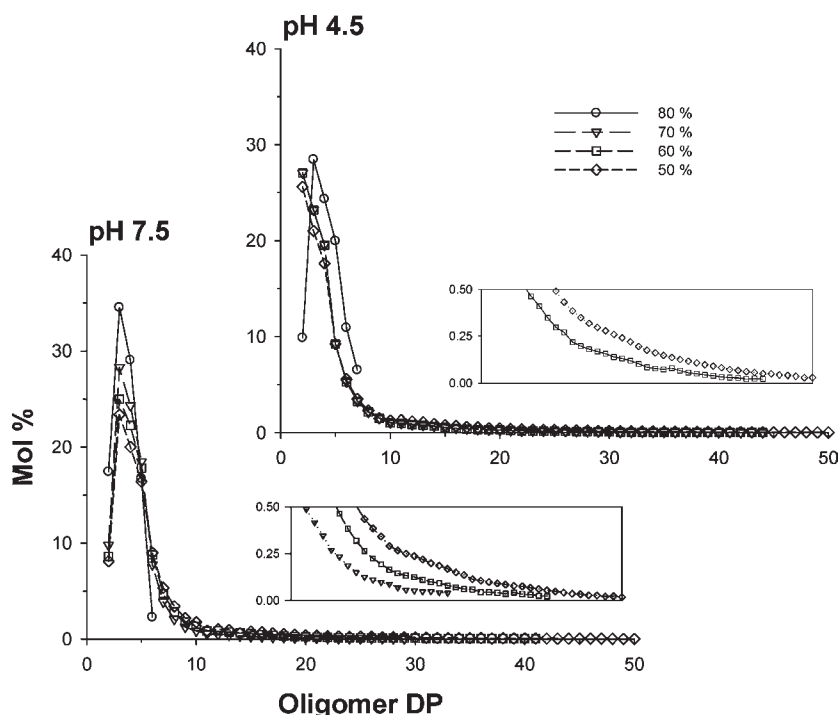


Figure 4. Experimentally measured average unmethylated oligogalacturonide distributions obtained following limited digestion of TT-PME-generated substrates with EPG.

Table 1. Effect of Demethylation pH and Degree of Polymerization on the Average Length of the Longest Demethylated Block Released by EPG and Observed by HPAEC–ELSD^a

pectin series (% DM)	oligomer DP	
	pH 7.5	pH 4.5
80	6 (79.9%)	7 (80.9%)
60	41 (60.0%)	45 (60.1%)
50	53 (50.0%)	57 (50.3%)

^a Numbers in parentheses are the DM value based on the actual amount of base added during demethylation.

Table 2. Comparison of C_n for pH 7.5 and 4.5 Demethylated Pectins^a

oligomer DP	degree of methylation		
	80%	60%	50%
3	NS ^b	c	c
4	NS ^b	d	e
5	e	f	e
6	d	c	c

^a Means were compared using Student's *t* test (one-tailed) assuming unequal variances. ^b NS = not significant. ^c $p < 0.05$. ^d $p < 0.01$. ^e $p < 0.005$. ^f $p < 0.001$.

did not increase with a decrease in DM, as might be anticipated if high levels of secondary fragmentation occurred. Additionally, extended digests with EPG resulted in the disappearance of peaks associated with large oligogalacturonides and increased peak areas from monomer to tetramer (data not shown). Although not as well characterized as *Aspergillus niger* EPGs, the resulting

Table 3. Sum of DMB per Molecule (\bar{B}), Average DMB Size (\bar{BS}), and Number of Average Size DMB per Molecule (\bar{BN})^a

DM	\bar{B}		\bar{BS}		\bar{BN}	
	pH 7.5	pH 4.5	pH 7.5	pH 4.5	pH 7.5	pH 4.5
80	6.3 a ^b	7.1 a	3.5 a ^c	3.6 a	1.8 a ^b	1.9 a
60	6.7 b ^d	6.9 ab	4.3 b ^c	5.8 b	1.5 b ^c	1.2 b
50	7.1 c ^e	5.8 c	4.4 c ^e	6.8 c	1.6 b ^c	0.8 c

^a Values within a column that have different letters indicate a significant difference ($p \leq 0.05$) based on analysis of variation (ANOVA) and Tukey's multiple comparison test. ^b Significant differences between means for pH pairs of each variable based on Student's *t* test; $p < 0.01$. ^c Significant differences between means for pH pairs of each variable based on Student's *t* test; $p < 0.001$. ^d Significant differences between means for pH pairs of each variable based on Student's *t* test; $p < 0.05$.

digestion patterns, produced when oligomers of DP 7–21 were treated with the commercial EPG used here, demonstrate a low rate of accumulation for DP 1–3 oligomers.³⁹

No oligomers with a DP larger than GalA₇ were released from the 80% DM pectins (Table 1 and Figure 4). Significant differences were observed when comparing the amount (nmol mL⁻¹) of oligomers released for GalA_n at pH 7.5 versus 4.5 for each pectin series (Table 2 for 80% DM series). For the 70% DM series, only GalA₃₇ and GalA₃₉ oligomers were not significantly different between the two pH treatments (Student's *t* test, one-tailed, assuming unequal variances; data not shown). Significant differences were observed for lower DP oligomers with the 50% DM series below DP 13, but from DP 14 to 53, only seven of the pH 7.5/4.5 pairs had *p* values below 0.05 (data not shown).

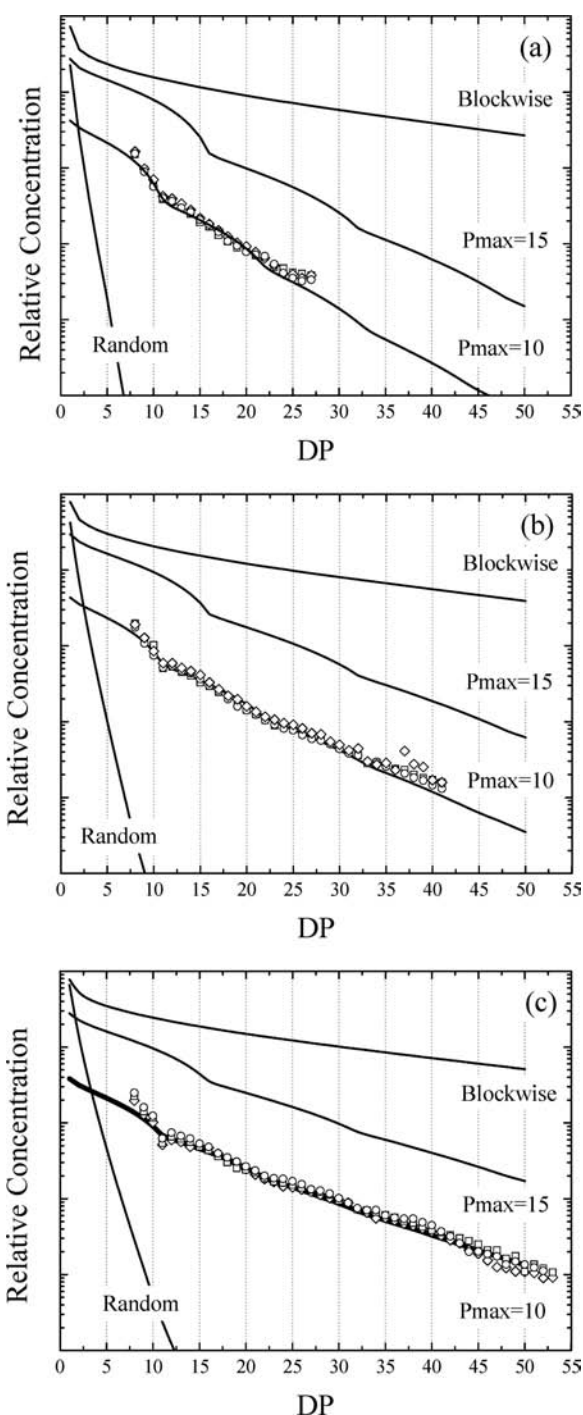


Figure 5. Distributions of oligogalacturonides predicted to be released by limited EPG digestions from HGs, generated from a 94% DM starting substrate using either random demethylesterification or PME models as described above, with maximum processivities of either greater than the DP of the chains (“completely blockwise”) or 15 and 10 residues compared to experimental data (three independent experiments at pH 7.5) for final sample averaged DMs of (a) 70%, (b) 60%, and (c) 50%.

\bar{B} was estimated for each demethylated HG using the pooled slope (1.355 95) and intersect (6.205 08) data obtained from ANCOVA analysis of GalA₆ and GalA₁₃ calibration curves and the M_n estimated by SEC–MALLS (see eq 2). Statistically significant differences were present for \bar{B} in both pH series (Table 3). Trends associated with decreasing DM values differed

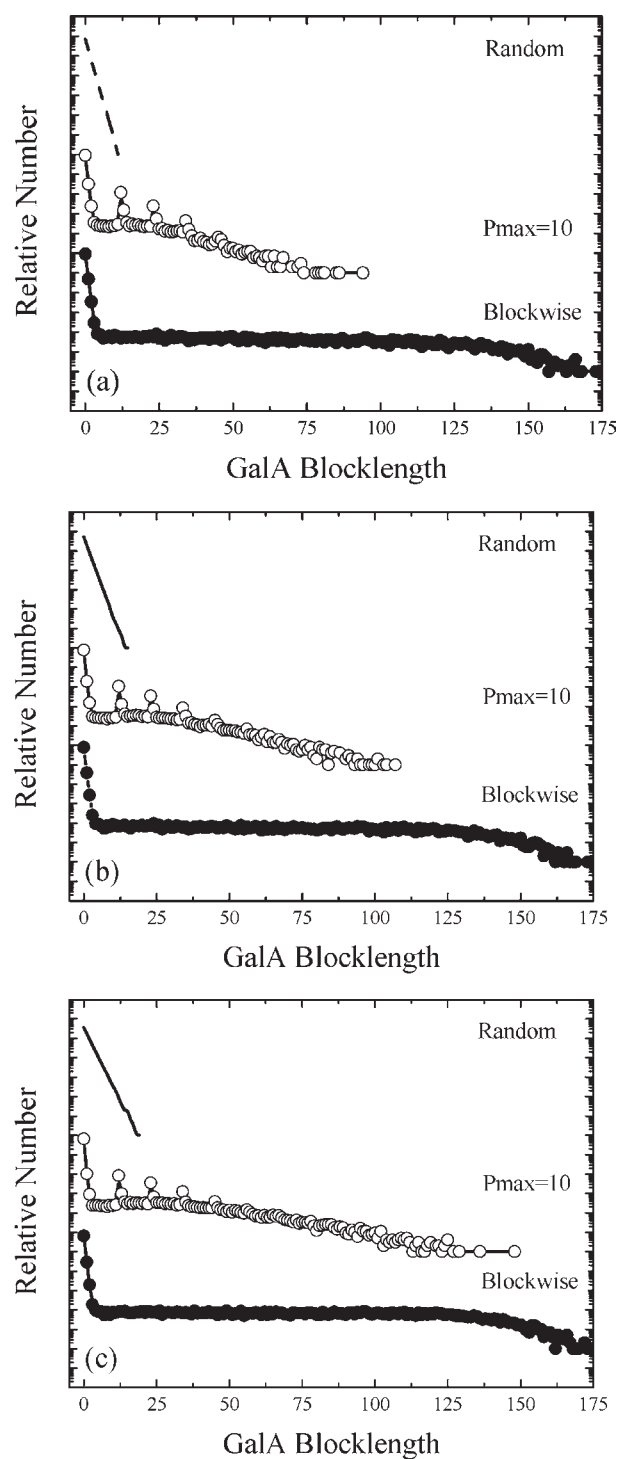


Figure 6. Full unmethylesterified GalA block length distributions for the TT-PME-modified samples at pH 7.5, obtained from the simulations that gave good agreement of the predicted and experimental oligomers released by the limited digest, for samples of (a) 70%, (b) 60%, and (c) 50% DM.

for the two pH series, with \bar{B} increasing at pH 7.5 but decreasing at pH 4.5. Comparisons showed the mean values at each DM at pH 7.5 versus 4.5 were also significantly different. Values for \bar{B} less than 1.0 suggest that not all molecules were acted on by the TT-PME enzyme. This has also been observed with the commercially available²¹ citrus SI-PME based on the calcium-sensitive

pectin ratio²⁰ and capillary electrophoresis electropherograms.³⁵ Significant differences were also present between pH 7.5 versus 4.5 DM pairs for \overline{BS} and \overline{BN} (Table 3) at each DM and for means within each pH series. Trends in \overline{BS} were similar for both pH treatments, although \overline{BS} estimates were significantly larger for the pH 4.5 series at each DM value (Table 3). Values reported here for \overline{BS} are smaller than those reported previously for the SI-PME^{19,35} for equivalent decreases in DM. Additionally, \overline{BS} was significantly larger in each DM pair when the demethylation occurred at pH 4.5 for TT-PME, while for SI-PME, \overline{BS} was larger in pH 7.5 demethylesterifications.¹⁹ As might be expected, the \overline{BN} estimates decrease as \overline{BS} increased, with greater reductions occurring in the pH 4.5 demethylated series (Table 3).

Panels a–c of Figure 5 show distributions of oligogalacturonides predicted to be released by limited EPG digestions of HGs of 70, 60, and 50% DM, generated from a 94% DM starting substrate using either random demethylesterification or PME models as described above. They illustrate maximum processivities of either greater than the DP of the chains (“completely blockwise”) or 15 and 10 residues. Also shown is the comparison of the equivalent experimental data to the PME model, with a maximum processivity of 10. In contrast to the citrus SI-PME,¹⁹ the oligogalacturonide distributions produced from the TT-PME demethylesterified samples, at both pH 7.5 and 4.5 and at all DM values investigated, conform to the simulated multiple-attack mechanism but additionally with a p of around 10. It should be noted that oligomers with a DP < 7 (as in the 80% DM samples) were not compared, because as a result of their size being smaller than that which can be accommodated in the EPG subsite architecture, the limited digest model employed is not expected to be a good approximation.²² Panels a–c of Figure 6 show the full unmethylesterified GalA block length distributions for the TT-PME-modified samples at pH 7.5, obtained from the simulations that gave good agreement of the predicted and experimental oligomers released by the limited digest, for samples of 70, 60, and 50% DM. The distributions for two alternative models are also shown to illustrate that large differences in the full GalA block length distributions exhibited by the generated HGs are predicted to exist if the enzyme functions in a different way. This highlights the need for careful mathematical modeling to generate faithful distributions *in silico* that can further be used to develop models of function.

Results presented here for citrus TT-PME and previously for citrus SI-PME¹⁹ suggest that the pectin nanostructure is amenable to enzymatic engineering to produce tailored structural/functional properties. These results also indicate that the PME mode of action is different for two PME isoforms purified from the same species. Previous results have also shown that reaction parameters can also influence the mode of action.^{19,30,40,41} Future work is needed to demonstrate how the frequency distribution of \overline{BS} can be controlled and how the frequency distribution of \overline{BN} can also be manipulated.

AUTHOR INFORMATION

Corresponding Author

*Telephone: +1-863-293-4133. Fax: +1-863-299-8678. E-mail: randall.cameron@ars.usda.gov.

Funding Sources

This research was supported in part by a Cooperative Research and Development Agreement with CPKelco, Inc. (58-3K95-61136).

ACKNOWLEDGMENT

We thank Steven W. Kauffman and Elena Branca for technical assistance.

ABBREVIATIONS USED

TT-PME, thermally tolerant pectin methylesterase; HPAEC, high-pressure anion-exchange chromatography; ELSD, evaporative light-scattering detector; SI-PME, salt-independent pectin methylesterase; HG, homogalacturonan; GalA, galacturonic acid; DM, degree of methylation; pPME, plant pectin methylesterase; EPG, endopolygalacturonase; DMB, demethylesterified block; p , degree of processivity; SEC–MALLS, size-exclusion–multi-angle laser light scattering; DP, degree of polymerization; M_w , weight average molecular weight; M_n , number average molecular weight; AGA, anhydrous galacturonic acid; fwhh, full width at half height

REFERENCES

- (1) Kunzek, H.; Kabbert, R.; Gloyna, D. Aspects of material science in food processing: Changes in plant cell walls of fruits and vegetables. *Z. Lebensm.-Unters. -Forsch. A* **1999**, *208*, 233–250.
- (2) Parker, C. C.; Parker, M. L.; Smith, A. C.; Waldron, K. W. Pectin distribution at the surface of potato parenchyma cells in relation to cell–cell adhesion. *J. Agric. Food Chem.* **2001**, *49*, 4364–4371.
- (3) Van Buren, J. P. The chemistry of texture in fruits and vegetables. *J. Text. Stud.* **1979**, *10*, 1–23.
- (4) Fraeye, L.; De Roeck, A.; Duvetter, T.; Verlent, I.; Hendrickx, M.; Van Loey, A. Influence of pectin properties and processing conditions on thermal pectin degradation. *Food Chem.* **2007**, *105*, 555–563.
- (5) Sila, D. N.; Doungla, E.; Smout, C.; Van Loey, A.; Hendrickx, M. Pectin fraction interconversions: Insight into understanding texture evolution of thermally processed carrots. *J. Agric. Food Chem.* **2006**, *54*, 8471–8479.
- (6) Van Buggenhout, S.; Messagie, I.; Maes, V.; Duvetter, T.; Van Loey, A.; Hendrickx, M. Minimizing texture loss of frozen strawberries: Effect of infusion with pectinmethylesterase and calcium combined with different freezing conditions and effect of subsequent storage/thawing conditions. *Eur. Food Res. Technol.* **2006**, *223*, 395–404.
- (7) Duvetter, T.; Sila, D. N.; Van Buggenhout, S.; Jolie, R.; Van Loey, A.; Hendrickx, M. Pectins in processed fruit and vegetables: Part I—Stability and catalytic activity of pectinases. *Compr. Rev. Food Sci. Food Saf.* **2009**, *8*, 75–85.
- (8) Van Buggenhout, S.; Sila, D. N.; Duvetter, T.; Van Loey, A.; Hendrickx, M. Pectins in processed fruits and vegetables: Part III—Texture engineering. *Compr. Rev. Food Sci. Food Saf.* **2009**, *8*, 105–116.
- (9) Thibault, J.-F.; Renard, C. M. G. C.; Axelos, M. A. V.; Roger, P.; Crepeau, M.-J. Studies of the length of homogalacturonic regions in pectins by acid hydrolysis. *Carbohydr. Res.* **1993**, *238*, 271–286.
- (10) Ralet, M.-C.; Crepeau, M.-J.; Lefebvre, J.; Mouille, G.; Hofte, H.; Thibault, J.-F. Reduced number of homogalacturonan domains in pectins of an *Arabidopsis* mutant enhances the flexibility of the polymer. *Biomacromolecules* **2008**, *9*, 1454–1460.
- (11) Hellin, P.; Ralet, M.-C.; Bonnin, E.; Thibault, J.-F. Homogalacturonans from lime pectins exhibit homogeneous charge density and molar mass distributions. *Carbohydr. Polym.* **2005**, *60*, 307–317.
- (12) Ridley, B. L.; O'Neill, M. A.; Mohnen, D. Pectins: Structure, biosynthesis, and oligogalacturonide-related signaling. *Phytochemistry* **2001**, *57*, 929–967.
- (13) Laurent, M. A.; Boulenger, P. Stabilization mechanism of acid dairy drinks (ADD) induced by pectin. *Food Hydrocolloids* **2003**, *17*, 445–454.
- (14) Willats, W. G.; Orfila, C.; Limberg, G.; Buchholt, H. C.; van Alebeek, G. J.; Voragen, A. G.; Marcus, S. E.; Christensen, T. M.; Mikkelsen, J. D.; Murray, B. S.; Knox, J. P. Modulation of the degree and pattern of methyl-esterification of pectic homogalacturonan in plant cell

walls. Implications for pectin methyl esterase action, matrix properties, and cell adhesion. *J. Biol. Chem.* **2001**, *276*, 19404–19413.

(15) Boland, A. B.; Delahunty, C. M.; van Ruth, S. M. Influence of the texture of gelatin gels and pectin gels on strawberry flavour release and perception. *Food Chem.* **2006**, *96*, 452–460.

(16) Lubbers, S.; Decourcelle, N.; Martinez, D.; Guichard, E.; Tromelin, A. Effect of thickeners on aroma compound behavior in a model dairy gel. *J. Agric. Food Chem.* **2007**, *55*, 4835–4841.

(17) Patel, M.; Shah, T.; Amin, A. Therapeutic opportunities in colon-specific drug-delivery systems. *Crit. Rev. Ther. Drug* **2007**, *24*, 147–202.

(18) Madziva, H.; Kailasapathy, K.; Phillips, M. Evaluation of alginate–pectin capsules in Cheddar cheese as a food carrier for the delivery of folic acid. *Lebensm.-Wiss. Technol.* **2006**, *39*, 146–151.

(19) Cameron, R. G.; Luzio, G. A.; Goodner, K.; Williams, M. A. K. Demethylation of a model homogalacturonan with a salt-independent pectin methyl esterase from citrus: I. Effect of pH on demethylated block size, block number and enzyme mode of action. *Carbohydr. Polym.* **2008**, *71*, 287–299.

(20) Luzio, G. A.; Cameron, R. G. Demethylation of a model homogalacturonan with the salt-independent pectin methyl esterase from citrus: II. Structure function analysis. *Carbohydr. Polym.* **2008**, *71*, 300–309.

(21) Savary, B. J.; Hotchkiss, A. T.; Cameron, R. G. Characterization of a salt-independent pectin methyl esterase purified from Valencia orange peel. *J. Agric. Food Chem.* **2002**, *50*, 3553–3558.

(22) Hunt, J. J.; Cameron, R.; Williams, M. A. K. On the simulation of enzymatic digest patterns: The fragmentation of oligomeric and polymeric galacturonides by endo-polygalacturonase II. *Biochim. Biophys. Acta* **2006**, *1760*, 1696–1703.

(23) Cameron, R. G.; Baker, R. A.; Grohmann, K. Multiple forms of pectinmethyl esterase from citrus peel and their effects on juice cloud stability. *J. Food Sci.* **1998**, *63*, 253–256.

(24) Cameron, R. G.; Savary, B. J.; Hotchkiss, A. T.; Fishman, M. L. Isolation, characterization, and pectin-modifying properties of a thermally tolerant pectin methyl esterase from *Citrus sinensis* var. Valencia. *J. Agric. Food Chem.* **2005**, *53*, 2255–2260.

(25) Versteeg, C.; Rombouts, F. M.; Spaansen, C. H.; Pilnik, W. Thermostability and orange juice cloud destabilizing properties of multiple pectinesterases from orange. *J. Food Sci.* **1980**, *45*, 969–971.

(26) Cameron, R. G.; Grohmann, K. Partial purification and thermal characterization of pectinmethyl esterase from red grapefruit finisher pulp. *J. Food Sci.* **1995**, *60*, 821–825.

(27) Seymour, T. A.; Preston, J. F.; Wicker, L.; Lindsay, J. A.; Marshall, M. R. Purification and properties of pectinesterases of Marsh white grapefruit pulp. *J. Agric. Food Chem.* **1991**, *39*, 1075–1079.

(28) Grohmann, K.; Cameron, R. G.; Buslig, B. S. Fractionation and pretreatment of orange peel by dilute acid hydrolysis. *Bioresour. Technol.* **1995**, *54*, 129–141.

(29) Cameron, R. G.; Grohmann, K. Separation, detection and quantification of galacturonic acid oligomers with a degree of polymerization greater than 50. *J. Liq. Chromatogr. Relat. Technol.* **2005**, *28*, 559–570.

(30) Catoire, L.; Pierron, M.; Morvan, C.; Herve du Penhoat, C.; Goldberg, R. Investigation of the action patterns of pectinmethyl esterase isoforms through kinetic analyses and NMR spectroscopy. *J. Biol. Chem.* **1998**, *273*, 33150–33156.

(31) Daas, P. J. H.; Meyer-Hansen, K.; Schols, H. A.; De Ruyter, G. A.; Voragen, A. G. J. Investigation of the non-esterified galacturonic acid distribution in pectin with endopolygalacturonase. *Carbohydr. Res.* **1999**, *318*, 135–145.

(32) Limberg, G.; Korner, R.; Buchholt, H. C.; Christensen, T. M.; Roepstorff, P.; Mikkelsen, J. D. Quantification of the amount of galacturonic acid residues in blocksequences in pectin homogalacturonan by enzymatic fingerprinting with exo- and endo-polygalacturonase II from *Aspergillus niger*. *Carbohydr. Res.* **2000**, *327*, 321–322.

(33) Limberg, G.; Korner, R.; Buchholt, H. C.; Christensen, T. M. I. E.; Roepstorff, P.; Mikkelsen, J. D. Analysis of different de-esterification

mechanisms for pectin by enzymatic fingerprinting using endopolygalacturonase II and endopolygalacturonase II from *A. niger*. *Carbohydr. Res.* **2000**, *327*, 293–307.

(34) Ralet, M.-C.; Thibault, J. F. Interchain heterogeneity of enzymatically deesterified lime pectins. *Biomacromolecules* **2002**, *3*, 917–925.

(35) Williams, M. A. K.; Cucheval, A.; Nasser, A. T.; Ralet, M.-C. Extracting intramolecular sequence information from intermolecular distributions: Highly nonrandom methylester substitution patterns in homogalacturonans generated by pectinmethyl esterase. *Biomacromolecules* **2010**, *11*, 1667–1675.

(36) Rosenbohm, C.; Lundt, I.; Christensen, T. I. E.; Young, N. G. Chemically methylated and reduced pectins: Preparation, characterization by ¹H NMR spectroscopy, enzymatic degradation, and gelling properties. *Carbohydr. Res.* **2003**, *338*, 637–649.

(37) Benen, J. A. E.; Kester, H. C. M.; Visser, J. Kinetic characterization of *Aspergillus niger* N400 endopolygalacturonases I, II and C. *Eur. J. Biochem.* **1999**, *259*, 577–585.

(38) Chen, E. M. W.; Mort, A. J. Nature of sites hydrolyzable by endopolygalacturonase in partially-esterified homogalacturonans. *Carbohydr. Polym.* **1996**, *29*, 129–136.

(39) Cameron, R. G.; Luzio, G. A.; Savary, B. J.; Nunez, A.; Goodner, K. Digestion patterns of two commercial endopolygalacturonases on polygalacturonate oligomers with a degree of polymerization from 7–21. *Proc. Fla. State Hort. Soc.* **2009**, *122*, 295–302.

(40) Goldberg, R.; Pierron, M.; Bordenave, M.; Breton, C.; Morvan, C.; du Penhoat, C. H. Control of mung bean pectinmethyl esterase isoform activities. Influence of pH and carboxyl group distribution along the pectic chains. *J. Biol. Chem.* **2001**, *276*, 8841–8847.

(41) Kim, Y.; Teng, Q.; Wicker, L. Action pattern of Valencia orange PME de-esterification of high methoxyl pectin and characterization of modified pectins. *Carbohydr. Res.* **2005**, *340*, 2620–2629.